Journal of Metals, Materials and Minerals, 35(3), e2354, 2025

Bagasse lignin for single-used food packaging applications: UV-barrier, antioxidant, migration and cytotoxicity

Pawarisa WIJARANAKUL[1], Bongkot HARARAK[1,*], Wanwitoo WANMOOLEE[2], Prapudsorn WANNID[1], and Weerawan LAOSIRIPOJANA[3]

[1] *National Metal and Materials Technology Center (MTEC), National Science and Technology Development Agency, 114 Thailand Science Park, Khlong Luang, Pathum Thani, 12120, Thailand*

[2] *Department of Chemical Engineering, Faculty of Engineering, King Mongkut's University of Technology North Bangkok (KMUTNB), Bangkok, 10800, Thailand*

[3] *Department of Tool and Materials Engineering, Faculty of Engineering, King Mongkut's University of Technology Thonburi (KMUTT), Bangkok, 10140, Thailand*

***Corresponding author e-mail**: bongkoth@mtec.or.th

Received date:
11 March 2025
Revised date:
4 May 2025
Accepted date:
1 June 2025

Keywords:
PLA bio composites;
Sugarcane bagasse lignin;
UV shielding

Abstract

This study examined PLA biocomposite films made from organosolv lignin extracted from Thai agro-waste, specifically sugarcane bagasse (BG), to assess their suitability for food packaging, focusing on their physical, thermal, optical, UV-shielding, antioxidant, and migration properties. Extracted BG-lignin exhibited free radical scavenging ability with an EC50 value of 400 $\mu g \cdot mL^{-1}$, reducing DPPH absorbance by 50%. PLA composite films with BG-lignin dosage from 0.1 to 1.0 wt% were successfully fabricated via conventional blown film extrusion. Addition of BG-lignin at 0.5 wt% and 1.0 wt% to PLA films decreased UV transmittance from 90% to 30% and 12%, respectively, without compromising optical clarity. Moreover, DPPH scavenging activity of all composite films with different BG-lignin contents (0.1 wt% to 1.0 wt%) reached 50% within 24 h, while overall migration values and cytotoxicity level are below the permissible limit. This study demonstrates the potential application of PLA/BG-lignin composite films for single-used ketchup sachets. These films effectively reduce ketchup color change under UV light exposure.

1. Introduction

The annual plastic food packaging of 170 million tons constitutes the largest end-user market, representing nearly 40% of the global demand for synthetic plastics [1,2]. However, mismanagement of the single-used plastic packaging contributes significantly to environmental degradation, adversely impacting ecosystems, marine life, and human health. Urgent action is required to address this issue by transitioning alternative biodegradable and eco-friendly packaging materials.

Bio-based and biodegradable plastics have emerged as promising alternatives for single-used food packaging applications. An example of such a material is poly (lactic acid) (PLA), a polyester commercially produced from renewable plant sources. PLA has good melt viscosity and can be fabricated through conventional blown film melt-extrusion processes [3]. PLA film has high transparency, with mechanical properties suitable for film packaging applications. However, PLA is not suitable for UV-sensitive products as it has poor UV light absorption [4]. To improve UV protection without sacrificing eco-friendliness, a range of natural fillers such as cellulose [5,6], starch [7] and lignin [8,9] have been incorporated into the PLA matrix. However, using cellulose and starch damage film transparency. In addition to transparency, cellulose and starch also present challenges related to poor thermal stability and difficult dispersion in polymer matrices, which often complicate film processability [10]. In contrast, lignin offers better UV-shielding and thermal resistance while maintaining acceptable film transparency at low loading levels [11,12].

Lignin is particularly intriguing due to its abundant availability and aromatic structure. Phenolics, unconjugated carbonyl, methoxyl and other chromophore groups in lignin can absorb UV light in the range 250 nm to 400 nm [13-15]. The chemical compositions and functional groups present in lignin are influenced by various factors, including the botanical source, environmental conditions during growth, and methods of extraction [16-18]. Lignin is comprised of three main monomeric units: p-coumaryl, coniferyl, and sinapyl alcohols. These mono-lignols play a role in the creation of lignin units, which are referred to as p-hydroxyphenyl (H), guaiacyl (G), and syringyl (S) units, respectively. Softwood is predominantly composed of G units, while hardwood comprises both S and G units with traces of H units. Herbaceous types, such as sugarcane bagasse, corncob, and wheat straw, consist of all three mono-lignols (H, G, and S) [19].

Sugarcane bagasse is a by-product of the sugar industry and can be used to produce second-generation (2G) bio-ethanol [20]. In Thailand, approximately 100 million tons of sugarcane are used annually by the sugar industry [21]. Bagasse is generated as a by-product after sugar manufacturing and accounts for approximately 28% of the sugarcane. Dried bagasse is composed of approximately 40% to 45% cellulose,

30% to 35% hemicellulose, and 20% to 30% lignin [21]. Therefore, 7×10^9 kg to 8×10^9 kg of lignin are available each year in Thailand. Industrial lignin extraction methods include sulfur and sulfur-free processes. Organosolv techniques, using solvents like ethanol, offer higher purity and lower ash content compared to other methods due to their safety, simplicity, and cost-effectiveness [22].

Various lignin types have been employed as multifunctional additives in PLA to enhance antimicrobial, antioxidant, and UV-barrier properties [8,9,23-26]. Kraft lignins, both pristine and chemically modified, improved UV-barrier properties of PLA films [25]. Corncob lignin addition enhanced antioxidation ability and UV-barrier properties of PLA [8]. Soda lignin, after fractionation and grafting with l-lactide, significantly improved UV-barrier properties compared to lignin-g-PLA composites [23]. Moreover, PLA/lignin composites at a lignin content of 40 wt% have been studied for active functions and monitored for overall migration, crucial for food packaging. Attained films containing softwood kraft lignin and esterified softwood lignin demonstrated migration values below the European standard limit (60 mg·kg^{-1}) [8].

To the best of our knowledge, there is no existing literature discussing the physicochemical properties relevant to food packaging applications of organosolv lignin obtained from sugarcane bagasse. This study investigates the physicochemical properties of BG-lignin, including chemical composition, thermal behavior, and free radical scavenging. Additionally, essential properties of PLA/BG-lignin composite films, such as color, thermal stability, and tensile strength, were evaluated. Active functions for food packaging applications, including UV-barrier, antioxidation, overall migration and cytotoxicity were also examined. Furthermore, this research demonstrates the potential application of the produced PLA/BG-lignin composite films for preventing photooxidation in ketchup sachets.

2. Experimental

2.1 Materials

BG-lignin was generously provided by the Biorefinery and Biological Technology Research Group at the National Center for Genetic Engineering and Biotechnology (BIOTEC). The PLA grade 4043D was supplied by NatureWorks LLC, with a number-average molecular weight (Mn) of 160,000 g·mol^{-1}, D content at 4%, and a melt flow rate of 6.0 g·10 min^{-1} at 210°C. 2,2-Diphenyl-1-picrylhydrazyl (DPPH), butylated hydroxytoluene (BHT), and dimethyl sulfoxide (DMSO) were procured from Sigma Aldrich. Ketchup sample is manufactured by Roza (Hi-Q Food products company, Thailand).

2.1.2 Characterizations of BG-lignin

2.1.2.1 Scanning Electron Microscopy (SEM)

The size and shape of bagasse-derived lignin (BG-lignin) particles were analyzed using a field-emission scanning electron microscope (FE-SEM, Hitachi SU5000, Japan). The lignin powder was first placed onto a standard SEM stub, dried at 40°C for 12 h to remove moisture, and coated with a thin layer of platinum using a Quorum Q150RS sputter coater (UK) at 15 mA for 60 s to enhance conductivity and image resolution.

2.1.2.2 Gel Permeation Chromatography (GPC)

The gel permeation chromatography (GPC) analysis of BG-lignin involved the use of a Waters e2695 separation module in the USA to determine both its molecular weight and molecular weight distribution. For this analysis, a 10 mg sample of extracted BG-lignin was dissolved in 3 mL of tetrahydrofuran (THF) and stirred at room temperature (approximately 32°C) for 12 h to achieve a homogeneous solution. The solution was filtered using nylon 66 membrane (pore size 0.2 mm) and 100 mL of the filtered solution was injected into the GPC column with flow rate of 1.0 mL·min^{-1} at 35°C. A series of narrow polystyrene standards were used for this calibration.

2.1.2.3 Fourier Transform Infrared Spectroscopy (FTIR)

Fourier transform infrared spectroscopy (FTIR) was conducted for qualitative characterization of chemical groups and key monolignols in BG-lignin using the transmission mode of a Thermo Scientific Nicolet 870 Spectrometer, USA. Pre-dried BG-lignin, weighing 1.5 mg, was blended with 200 mg of potassium bromide and subsequently compressed into a 13.0 mm disk. FTIR spectra were obtained by averaging 100 scans at a resolution of 4 cm^{-1} over the wavenumber range of 4000 cm^{-1} to 600 cm^{-1}.

2.1.2.4 ^{31}P Nuclear Magnetic Resonance (^{31}P NMR)

Phosphorus-31 nuclear magnetic resonance spectroscopy (31P NMR) was performed using an AV-500 Bruker Biospin instrument located in the United States to assess both the qualitative and quantitative chemical compositions of BG-lignin. The lignin solution preparation method adhered to the procedures outlined in a previously published Nature article [27]. Solvent A was a blend of anhydrous pyridine and CDCI3 in a ratio of 1.6:1 (v/v). An internal standard was created by combining 5.0 mg of chromium (III) acetylacetonate and 18.0 mg of N-hydroxy-5-norbornene-2,3-dicarboximide (NHND) with 1.0 mL of solvent A. Pre-dried lignin (30 mg), 0.1 mL of the internal standard, and 0.5 mL of solvent mixture A were mixed and stirred overnight to ensure complete dissolution of the lignin particles. Subsequently, 0.1 mL of the phosphitylation reagent TMDP (2-chloro-4,4,5,5-tetramethyl-1,3,2-dioxaphospholane) was added and stirred for 30 s, facilitating the transfer of the phosphitylated lignin solution into the NMR tube for subsequent analysis using Bruker Topspin software. The analysis was conducted at 295 K with a frequency of 500 MHz, 256 scans, and a relaxation delay time of 5 s.

2.1.2.5 Differential Scanning Calorimetry (DSC)

Glass transition temperature (Tg) of BG-lignin was measured by differential scanning calorimetry (DSC) (DSC-1, Mettler Toledo, Switzerland). Approximately 8 mg of BG-lignin was placed in a 40 mL aluminum pan. The specimen was heated from 40°C to 105°C and kept isothermal for 5 min for moisture removal. Then, it was gradually cooled to 40°C and reheated again to 200°C with a heating rate of 10°C·min^{-1}.

2.1.2.6 DPPH antioxidant activity

Free radical scavenging activity of BG-lignin was determined using 2,2-diphenly-1-picrylhydrazyl (DPPH), with measurements carried out following the protocol proposed by Araújo *et al*. 2022 [28]. Briefly, 0.5 mM of DPPH in ethanol was prepared as the stock solution. BG-lignin was dissolved in dimethyl sulfoxide (DMSO) at different concentrations within the range of 100 µg·mL^{-1} to 1000 µg·mL^{-1}. Aliquots of 0.5 mL of lignin solutions were added to 3 mL of DPPH stock solution. The attained solutions were incubated for 30 min at room temperature under the absence of light before loading into a quartz cuvette (1 cm pathlength). Absorbances were determined using a Perkin Elmer Lambda model 950, USA and ethanol was used as the equipment blank. The absorbance at 517 nm was assigned to the characteristic of DPPH. The DPPH scavenging activity was determined by the following Equation (1) [29].

$$\text{DPPH scavenging activity (\%)} = \frac{A_{DPPH} - A_{sample}}{A_{DPPH}} \times 100 \quad (1)$$

where ADPPH is the absorbance of the DPPH stock solution and Asample is the absorbance of the BG-lignin. The effective concentration at which 50% DPPH (EC50) of BG-lignin was reported was compared to butylated hydroxytoluene (BHT) as a standard antioxidant.

2.2 Fabrication of PLA composite films containing BG-lignin

Figure 1 shows a schematic illustration of the fabrication process used to produce PLA/BG-lignin composite films. PLA pellets were blended with 2 wt% of BG-lignin powder and introduced into a single-screw extruder (Thermo-Haake Rheomix OS, Germany) fitted with a rod die (3 mm die diameter). The extruder barrel temperature was set at 170°C, 180°C, and 185°C, while the die temperature was maintained at 180°C. The screw rotation speed remained constant at 60 rpm throughout the process. The resulting extrudates of BG-lignin/PLA were passed through a water bath and then cut into 3 mm pellets. After that, immaculate PLA was added to these pellets in order to get the appropriate BG-lignin loading contents (0.1 wt%, 0.2 wt%, 0.5 wt%, and 1 wt%). The same single-screw extruder, fitted with a blown film die (34 mm inner die diameter and 1 mm die gap), was used to produce BG-lignin/PLA composite films. The film had a flat surface and a thickness of 13 cm and 35 µm, respectively, when the screw speed was kept at 60 rpm.

2.2.1 Characterizations of PLA/BG-lignin composite films

2.2.1.1 Color measurement

The surface color of neat PLA and PLA/BG-lignin composite films was evaluated using a Datacolor 650 spectrophotometer (Pakistan), operating under the CIELAB color space system. Three chromatic coordinates L* (lightness), a* (green to red), and b* (blue to yellow) were recorded from three independent measurements for each sample. The average values were used for analysis.

2.2.1.2 Mechanical properties

In compliance with ASTM D882 guidelines, an Instron 4502 series universal testing equipment was used to assess the composite films' tensile strength, Young's modulus, and elongation at break. Film specimens were conducted with gauge length and width of 50 mm and 15 mm, respectively. Crosshead speed was constant at 500 mm·min^{-1}. At least ten samples were taken and reported as averaged values, including the standard deviation (SD) number. The data underwent analysis through one-way analysis of variance (ANOVA) using Minitab ®19.2020.1 (64-bit) software by Minitab Inc., USA. Subsequently, comparisons were made utilizing Duncan's multiple range test, with significance set at a p-value of 0.05 (95% confidence interval).

2.2.1.3 Morphological analysis (SEM)

The morphology of PLA and PLA/BG-lignin composite films was investigated using scanning electron microscopy (SEM). Film specimens were first conditioned at room temperature and then cryo-fractured by immersing them in liquid nitrogen to create a clean and brittle fracture surface. This method was applied to obtain cross-sectional views along the machine direction, ensuring minimal deformation during fracturing. Following cryo-fracturing, the fractured surfaces were mounted onto SEM stubs using carbon adhesive tape. To prevent charging during imaging and to enhance surface conductivity, all samples were sputter-coated with a thin platinum layer (15 mA, 60 s) using a Quorum Q150RS sputter coater (Quorum Technologies, UK). The coated samples were then observed under a Hitachi SU5000 field-emission scanning electron microscope (FE-SEM, Japan) at an accelerating voltage appropriate for polymer composites

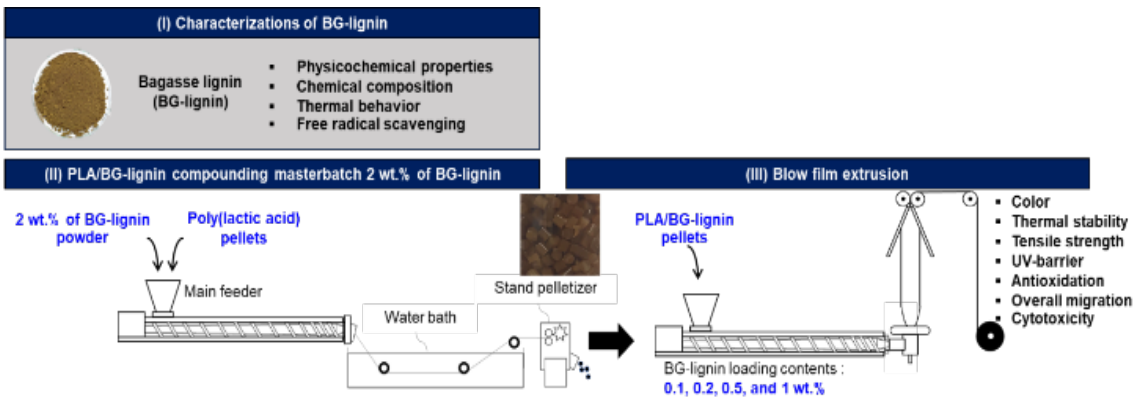

Figure 1. Schematic illustration of the fabrication process used to produce PLA/BG-lignin composite films.

2.2.1.4 UV-Visible Spectroscopy and Transparency

UV and visible light transmittance of all prepared films were measured using a UV-visible spectrometer (Perkin Elmer Lambda 950, USA) with a scanning range of 200 nm to 800 nm. Film transparency was measured using the method described by Cazón *et al*. and Terzioğlu *et al*. [30,31]. The following formula Equation (2), where x is the film thickness (mm) and $\%T_{600}$ is the transmission at 600 nm wavelength, was used to determine the transparency of the films.

$$\text{Transparency} = \frac{\log(\%T_{600})}{x} \quad (2)$$

2.2.1.5 Antioxidant activity (DPPH Assay)

Antioxidant capacity of both neat PLA and its BG-lignin composite films was determined using the DPPH free radical scavenging method. The measurements were performed in accordance with the guidelines put forward by Valencia *et al*. and Crouvisier-Urion *et al*. [32,33]. DPPH solution at a concentration of 50 $mg{\cdot}L^{-1}$ was prepared and kept in darkness. Then, 100 mg of the film was immersed in 10 ml DPPH solution contained in a UV-shielded sample vial. The mixture was stirred and kept at room temperature in darkness for 1 h, 5 h, 10 h, 20 h, and 24 h. The same ultraviolet-visible (UV-vis) spectrophotometer that was described in the section on the characterization of BG-lignin was used to measure the absorbance of DPPH at 517 nm. The DPPH scavenging activity was measured following Equation (1).

2.2.1.6 Overall migration testing

Overall migration tests of BG-lignin/PLA biocomposite films were conducted in accordance with Commission Regulation EU No 10/2011 and compared to neat PLA film. Rectangular strips of film samples with a total area of 10 cm^2 were prepared and fully submerged in sealed sample vials containing 10 mL of various simulants: simulant A (10%v/v ethanol) for aqueous food conditions, simulant B (3%w/v acetic acid) for acidic foods, simulant C (20%v/v ethanol) for alcoholic foods, simulant D1 (50%v/v ethanol) for milk products, and simulant D2 (N-heptane) for fatty food conditions. The samples were incubated in an oven at 40°C for 10 days, after which they were extracted, and the food simulants were dried at 105°C. The residue was weighed using a high-precision analytical balance (BOECO BAS 31 Plus, Germany) with ± 0.1 mg precision. Three replicates of each film were tested, and the average overall migration in $mg{\cdot}kg^{-1}$ was calculated and recorded. The absorbance of the corrected food simulant was analyzed by UV-vis spectrometry to confirm the presence of migrated lignin [34].

2.2.1.7 Cytotoxicity assessment

The effect of PLA/BG-lignin composite films on cell viability and cellular morphology was evaluated in accordance with ISO 10993-5. The films were subjected to in vitro cytotoxicity assessments, MTT cytotoxicity assay, using a conventional fibroblast cell culture (L929, Mouse Fibroblast Cells, ATCC CCL1, NCTC 929 of Strain L). The film samples were sterilized by UV irradiation for 15 min on each side. Thermanox coverslips and polyurethane film with 0.1% zinc diethyldithiocarbamate (ZDEC) were used as negative and positive control, respectively. The film's surface area-to-volume extraction ratio was maintained at 6 $cm^2{\cdot}mL^{-1}$ and a contact temperature of 37°C for a duration of 24 h. A microplate reader was used to detect absorbance at 570 nm. Percent of viability displayed in calculation form Equation (3), where OD570e is the mean value of the measured optical density of the 100% extracts of the test sample and OD570b is the mean value of the measured optical density of the 100% extracts of the blank.

$$\%\ \text{Viability} = 100 \times \frac{OD_{570e}}{OD_{570b}} \quad (3)$$

2.2.1.8 UV-Stability and color retention of packaged product

20 g of tomato ketchup were stored in consistent square-shaped neat PLA film and PLA/BG-lignin at 1.0 wt% film. These film packages were then positioned inside a UV chamber (ATLAS Suntest XLS+, USA) equipped with UV lamps emitting an irradiance of 50 $W{\cdot}m^{-1}$ within the wavelength range of 300 nm to 340 nm range. The UV chamber was kept in a controlled environment at 33°C for 72 h. The color change of the UV-exposed ketchup was measured every 12 h using a color spectrophotometer (Datacolor 650, Pakistan). Delta E (or ΔE), the color difference, was calculated in the change a CIE- L*, a* and b* system using the following Equation (4).

$$\Delta E = \sqrt{\left(L_i^* - L_0^*\right)^2 + \left(a_i^* - a_0^*\right)^2 + \left(b_i^* - b_0^*\right)^2} \quad (4)$$

In the provided equation, L_0^*, a_0^*, b_0^* represent the CIE L*, a*, and b* values of the ketchup before UV irradiation, while L_i^*, a_i^*, b_i^* represents the CIE L*, a*, and b* values of the UV-exposed ketchup at the sampling interval times.

3. Results and discussion

3.1 Characterizations of BG-lignin

Figure 2 shows SEM images of BG-lignin. At low magnification of 2000X (Figure 2(a)), BG-lignin presented as an accumulation of an innumerable amount of small particles, while irregular shapes and heterogeneity in particles size observed clearly at high magnification (Figure 2(b)). Quantitative particle size analysis revealed a broad size distribution ranging from 0.2 µm to 5 µm, supporting the visual observation of heterogeneity. The lignin particles were attached to each other due to self-agglomeration during the precipitation process. Similar morphological features and particle agglomeration behavior have been reported in previous studies, where lignin heterogeneity was attributed to broad molecular weight distributions and the lack of controlled fractionation during recovery processes [35].

The GPC technique, using THF as the eluent and polystyrene standard, determined the molecular weight of BG-lignin. The result revealed a broad normal distribution ranging from 300 $g{\cdot}mol^{-1}$ to 20,000 $g{\cdot}mol^{-1}$ (Figure S1), with an average Mw of 1638 $g{\cdot}mol^{-1}$ and a polydispersity index of 1.62, consistent with literature findings [22,36,37].

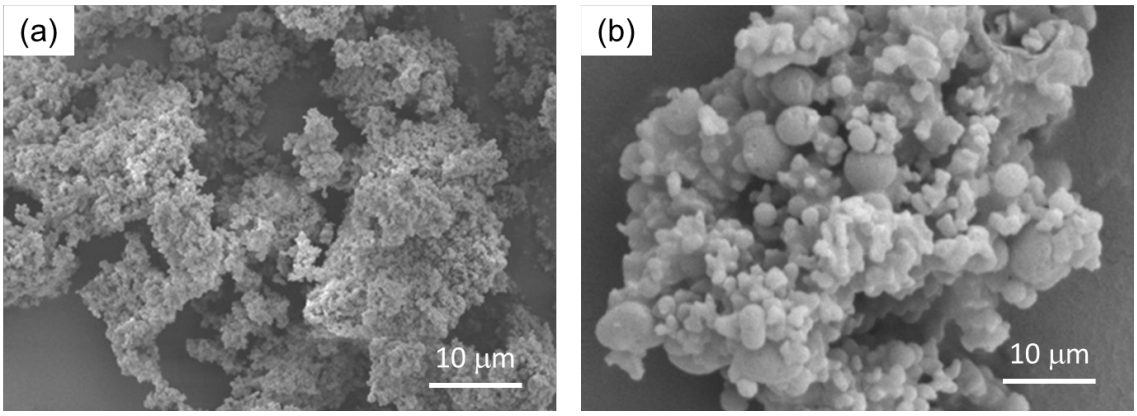

Figure 2. SEM micrographs of BG-lignin particles at (a) low (2000X) and (b) high (20000X) magnification.

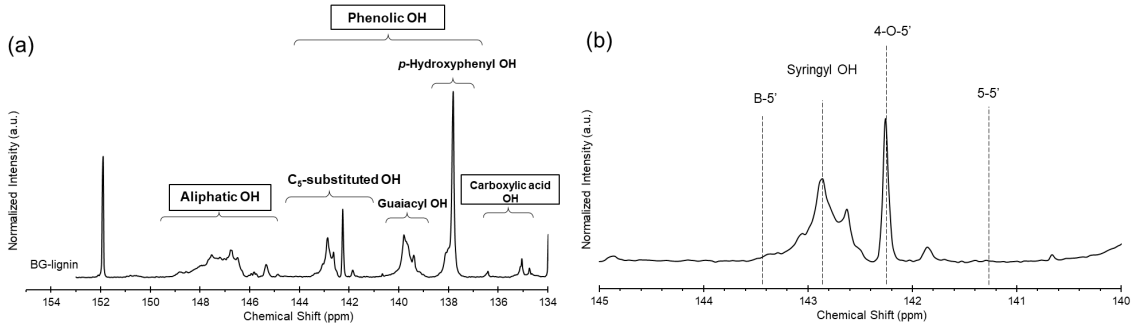

Figure 3. (a) ^{31}P-NMR spectra of BG-lignin with key signal assignments and (b) enlarged view at C_5-substituted hydroxyl.

Table 1. Quantification of hydroxyl and carboxyl groups in BG-lignin via ^{31}P NMR.

Sample	Aliphatic–OH	Phenolic–OH [mmol·g^{-1}]				COOH
	[mmol·g^{-1}]	C$_5$-substituted	Guaiacyl	Syringyl	p-hydroxyphenyl	[mmol·g^{-1}]
BG-lignin	1.43	1.06	0.60	0.38	0.95	0.45

The FTIR spectra of BG-lignin are displayed in Figure S2, with key functional groups assigned based on reported literature. Band assignments are summarized in Table S1. Figure S2(a) illustrates O–H stretching vibrations (3407 cm^{-1} to 3296 cm^{-1}), C–H stretching in CH_2 (2937 cm^{-1} to 2924 cm^{-1}) and CH_3 (2855 cm^{-1} to 2838 cm^{-1}), and C=O stretching (1695 cm^{-1} to 1712 cm^{-1}). The expanded fingerprint range (1800 cm^{-1} to 400 cm^{-1}) in Figure S2(b) reveals monolignol characteristics, including p-hydroxyphenyl (H), guaiacyl (G), and syringyl (S) vibrations. Specific vibrations observed in BG-lignin include aromatic skeleton vibration S>G (1425 cm^{-1}), C–H deformations in –CH_2– and –CH_3 (1460 cm^{-1}), aromatic skeletal vibrations (1425 cm^{-1}), aliphatic C–H stretch in CH_3 (1353 cm^{-1}), guaiacyl ring breathing (1257 cm^{-1}), and aromatic C–H in-plane deformation (G>S) (1031 cm^{-1}) [22,38].

A qualitative and quantitative assessment of the main monolignols in BG-lignin was conducted using 31P NMR based on the phosphitylation reaction, with NHND as the internal standard. The 31P NMR spectra of BG-lignin are presented in Figure 3. Three distinct types of hydroxyl groups—aliphatic, phenolic, and carboxylic—were identified, with chemical shifts ranging from 145.4 ppm to 150.0 ppm, 137.6 ppm to 144 ppm, and 133.6 ppm to 136.0 ppm, respectively. Table 1 compiled quantitative analysis involved integrating signal areas relative to the NHND internal standard. Phenolic hydroxyl was the main component in BG-lignin at 1.93 mmol·g^{-1}, with an aliphatic-to-phenolic hydroxyl ratio of 1.34. Within the phenolic hydroxyl region, p-hydroxyphenyl (H) at 137.5 ppm to 138 ppm, guaiacyl (G) at 139.4 ppm to 139.8 ppm, and syringyl (S) at 142.7 ppm were detected in BG-lignin, with contents of 0.95 mmol·g^{-1}, 0.60 mmol·g^{-1}, and 0.38 mmol·g^{-1}, respectively, resulting in an H:G:S ratio of 1:0.6:0.4. These findings are consistent with those reported for herbaceous biomass [22,36,39]. The types of phenolic hydroxyl groups in lignin depend on the native plant species [40], influencing UV-absorption, antioxidation, and antibacterial properties [41,42].

The glass transition temperature (Tg) of BG-lignin was evaluated by DSC, and the thermogram is shown in Figure S3. Two successive scans, including heating and cooling steps, were obtained after drying the BG-lignin sample at 105°C for 5 min under a nitrogen atmosphere to remove retained moisture. During the heating step, BG-lignin exhibited a single Tg representing an amorphous polymer at 110.3°C. After heating to 250°C, the sample was cooled, and the baseline indicated a reversed Tg of 135°C. This temperature was higher than the Tg observed in the heating thermogram due to thermal cross-linking during the heating step [43-47].

The antioxidant activity of lignin reported from various sources is closely linked to its chemical structure [16,17,48,49]. Structural characteristics, such as the presence of free phenolic hydroxyl and

methoxyl substitutions in aromatic rings, are key components influencing lignin's antioxidant activity. The antioxidant capability of BG-lignin based on DPPH scavenging was evaluated, with decreased absorbance of DPPH at 517 nm observed with increasing BG-lignin concentration, as shown in Figure 4(a), demonstrating its bio-antioxidant potential. The results compared the antioxidant ability of BG-lignin to that of the phenolic compound butylated hydroxytoluene (BHT), a common additive in both food and active food packaging [50,51]. Figure 4(b) illustrates the results of DPPH scavenging activity (%) of BHT and BG-lignin, showing an increase with higher BHT and BG-lignin content, reaching close to 90% when BHT content was 1000 $\mu g \cdot mL^{-1}$. The EC50 value, representing the concentration corresponding to 50% reduction of DPPH, was lower for BHT (75 $\mu g \cdot mL^{-1}$) than for BG-lignin (400 $\mu g \cdot mL^{-1}$). The EC50 value of BG-lignin used in this study was comparable to that reported for lignin extracted from bagasse in the literature [52,53].

3.2 Characterizations of PLA composite films containing BG-lignin

The appearance of the film is a crucial characteristic associated with PLA in food packaging applications. Color changes in film resulting from the inclusion of BG-lignin were quantified and documented using chromatic coordinates. The neat PLA film exhibited L*, a*, and b* values of 90.41, –0.52, and 11.51, respectively. Composite films containing BG-lignin exhibited a brownish that deepened to dark-brown with increasing BG-lignin content. Color changes were expressed as ΔL, Δa, and Δb, calculated relative to the neat PLA film and summarized in Table 2. The neat PLA film demonstrated the highest lightness value. An increase in BG-lignin content lead to reductions in both L* and a* while b* increased. For the highest loading content of 1.0 wt% (PLA/BG-lignin_1.0), the ΔL, Δa, and Δb values were recorded as –4.69, 1.48, and 7.50, respectively, confirmed the dark brown color film from BG-lignin dispersed in PLA film. The ΔL, Δa, and Δb values indicate how BG-lignin alters film appearance. A reduction in L* (lightness) and increases in a* (red/green) and b* (yellow/blue) suggest visible darkening and browning. These shifts can affect consumer perception, as films appearing overly dark or colored may not be acceptable for certain food products.

The mechanical properties of all films were assessed using ANOVA alongside Duncan's multiple range test, with a significance level set at $p < 0.05$. Figure 5 shows the mechanical properties tested along the machine direction (MD) and transverse direction (TD). Tensile strength in the MD significantly increased from 54.5 ± 4.5 MPa to 63 Mpa to 65 MPa when loading content of BG-lignin increased to 0.5 wt%. Tensile strength decreased to 56.6 ± 1.4 MPa when BG-lignin increased to 1.0 wt% which comparable to that of neat PLA film. Tensile strength in the TD decreased significantly when BG-lignin content was 1.0 wt% because high loading of BG-lignin restricted the arrangement of molecular chains along the TD. Young's modulus in both MD and TD of the BG-lignin/PLA composite films were similar with neat PLA. No significant differences in elongation at break tested in the MD direction were noticed, while adding BG-lignin at 1.0 wt% significantly reduced elongation at break. High loading content of lignin over 0.5 wt% resulted in deterioration of mechanical properties because of poor interaction and agglomeration of added lignin [24,54,55].

Morphology of the composite films and the interfacial adhesion between neat PLA and BG-lignin were investigated. Surface morphology by SEM of neat PLA film and its composite films at 5000x are shown in Figure S4. The neat PLA film displayed a smooth surface, while particles were evident on the surface of PLA/BG-lignin composite

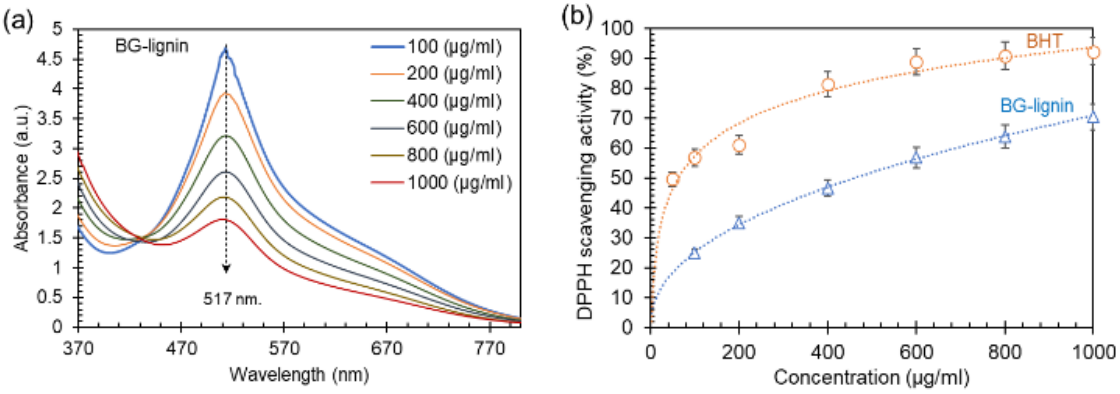

Figure 4. Free radical scavenging activity of BG-lignin, (a) absorbance of free radical DPPH at different concentrations of BG-lignin and (b) radical scavenging activity of BG-lignin and BHT.

Table 2. Color data of neat PLA film and PLA/BG-lignin composite films.

Sample	Std. CIE L*	Std. CIE a*	Std. CIE b*
Neat PLA	90.41	–0.52	11.51
PLA/BG-lignin composite films	ΔL	Δa	Δb
PLA/BG-lignin_0.1	–0.25	0.11	0.43
PLA/BG-lignin_0.2	–0.83	0.28	1.42
PLA/BG-lignin_0.5	–2.27	0.70	3.85
PLA/BG-lignin_1.0	–4.67	1.48	7.50

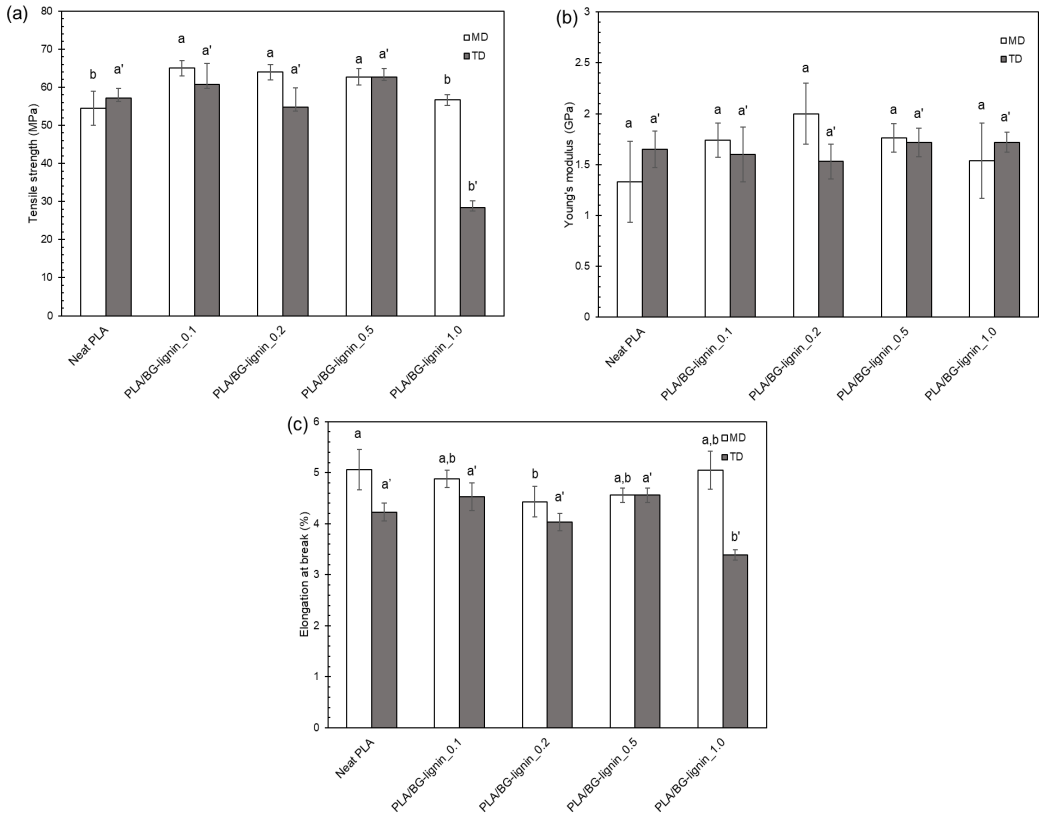

Figure 5. Mechanical properties of neat PLA film and its composites (a) tensile strength, (b) Young's modulus, and (c) elongation at break.

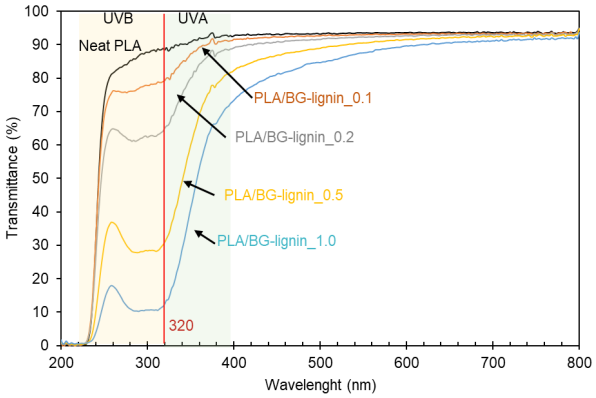

Figure 6. UV-visible spectra of neat PLA and PLA composite films with varying concentrations of BG-lignin (0.1 wt%, 0.2 wt%, 0.5 wt%, and 1.0 wt%).

films. At the highest BG-lignin level (1.0 wt%), the number of particles increased, good dispersion and no agglomeration were observed. Cross-sectional morphology was obtained from cryo-fractured surfaces of films frozen in liquid nitrogen. SEM images (Figure S5) revealed the morphology at both low (2000x) and high (10000x) magnifications, depicting overall thickness and the interface between PLA and BG-lignin. Neat PLA film exhibited a smooth fracture surface without inclusions, whereas incorporated BG-lignin particles were clearly visible in the composite films. At low magnification, well-dispersed BG-lignin particles were observed, consistent with the film surface morphology. At high magnification, gaps between BG-lignin particles and the PLA matrix were evident, indicating poor interfacial adhesion and decreased elongation at break of PLA composite films, particularly at a BG-lignin loading of 1.0 wt%

High optical transparency is crucial for food packaging, but allowing UV light to pass through the film can lead to oxidation reactions and color changes. Therefore, UV-blocking properties are important for film packaging. Lignin, with its chromophore groups, is a promising bio-UV absorber [25,26,56]. Transmission spectra in both UV and visible light for neat PLA film and BG-lignin/PLA composite films are shown in Figure 6. Neat PLA film exhibited almost complete transparency, with 90% transmittance in the visible region (400 nm to 800 nm) and high transmittance (90%) in the UV region, indicating insufficient UV-barrier property. PLA composite films with BG-lignin showed UV-shielding ability. At the highest loading lignin content (PLA/BG-lignin_1.0), transmission in both UVA (320 nm to 400 nm) and UVB (280 nm to 320 nm) regions significantly decreased compared to neat PLA film. UV transmittance at 320 nm, selected to evaluate UV-shielding ability, decreased with increasing BG-lignin content, from 79% to 12%. This UV absorption is attributed to the phenolic hydroxyl and other chromophore groups in BG-lignin, such as carbonyl and methoxy structures, which can absorb radiation in the 250 nm to 400 nm range [13,14,56,57].

The transparency of the neat PLA film was 53.3%. PLA composite films incorporated with BG-lignin showed similar transparencies of 52% to 53%, indicating that loading BG-lignin ranging from 0.1 wt% to 1.0 wt% did not significantly affect film transparency. The inclusion of a small amount of BG-lignin improved the UV absorption of PLA in the composite films while maintaining satisfactory transparency. Higher loading content of BG-lignin resulted in better UV-barrier properties, but darker film color was obtained. Thus, the loading content of BG-lignin and UV-barrier properties should be optimized for specific applications.

Oxidation is a significant cause of food deterioration, particularly in foods rich in lipids and bioactive compound [58]. Oxidation can be prevented by incorporating antioxidant compounds directly into food or by utilizing antioxidants in the packaging [59]. The most common synthetic antioxidants used in food packaging are butylated hydroxyanisole (BHA), butylated hydroxytoluene (BHT) and tert-butyl hydroquinone (TBHQ). However, regulations restrict the use of these synthetic antioxidants. BG-lignin, with an EC50 of 400 $\mu g \cdot mL^{-1}$, exhibits promising antioxidant properties for food packaging. DPPH scavenging activity was evaluated in PLA/BG-lignin composite films. Figure 7(a-c) depict the absorbance bands of neat PLA, PLA/BG-lignin_0.1, and PLA/BG-lignin_1.0 composite films. The absorbance band at 517 nm of the DPPH ethanolic solution declined over 24 h, reflecting strong antioxidant activity. Figure 7(d) illustrates the calculated percentages of DPPH scavenging activity over time. The DPPH scavenging activity of neat PLA film remained constant for the first 5 h, gradually increasing to a plateau value of 21% after 10 h. At 5 h, PLA composite films with 0.5 wt% and 1.0 wt% BG-lignin exhibited a notable increase in DPPH scavenging activity to approximately 14%, while films with lower BG-lignin contents (0.1 wt% and 0.2 wt%) showed comparable activity to neat PLA film. PLA/BG-lignin films reached 50% scavenging activity after 24 h, showing concentration and time-dependent behaviour. The antioxidant activity stems from the presence of phenolic hydroxyl groups, which act as hydrogen donors to stabilize free radicals. This is particularly relevant in solid films, where radical diffusion is slower compared to liquid systems [60].

The overall migration test with simulants representing aqueous and fatty food conditions revealed insightful findings, as summarized in Table 3. European legislation mandates a permissible overall migration limit of 60 $mg \cdot kg^{-1}$ for food packaging materials [8]. After a 10 day incubation period, migration values for neat PLA films in various simulants were measured. For simulant A (aqueous foods), simulant B (acidic foods), simulant C (alcoholic foods), simulant D1 (milk products), and simulant D2 (fatty foods), migration levels were 4.4 $mg \cdot kg^{-1}$, 7.4 $mg \cdot kg^{-1}$, 6.3 $mg \cdot kg^{-1}$, 6.6 $mg \cdot kg^{-1}$, and 5.3 $mg \cdot kg^{-1}$, respectively. Interestingly, the overall migration in 20% ethanol was lower than in 10% ethanol. This observation may be attributed to differences in polymer relaxation and swelling behavior; higher ethanol concentrations can sometimes reduce lignin diffusion due to matrix contraction or solvent polarity mismatch. Notably, the PLA composite film containing 1.0 wt% BG-lignin (PLA/BG-lignin_1.0) recorded a maximum migration value of 43 $mg \cdot kg^{-1}$. Despite this increase, it remained well below the regulatory threshold, suggesting the feasibility of using BG-lignin at a maximum loading of 1.0 wt% for food packaging. These findings underscore BG-lignin's potential as a PLA composite film additive without compromising regulatory compliance.

The absorbance of the corrected food simulant was analyzed by UV-vis spectrometry to confirm lignin migration. Absorbance at 280 nm indicates lignin presence [61]. Figure 8(a-b) show UV absorption of the food simulant after 10 days. Neat PLA film showed no absorbance at 280 nm, while a broad band was observed with 0.5 wt% and 1.0 wt% BG-lignin, confirming its leaching into the food simulants. Results of DPPH scavenging activity and overall migration suggest BG-lignin acted as a free radical scavenger, with migration below EU limits.

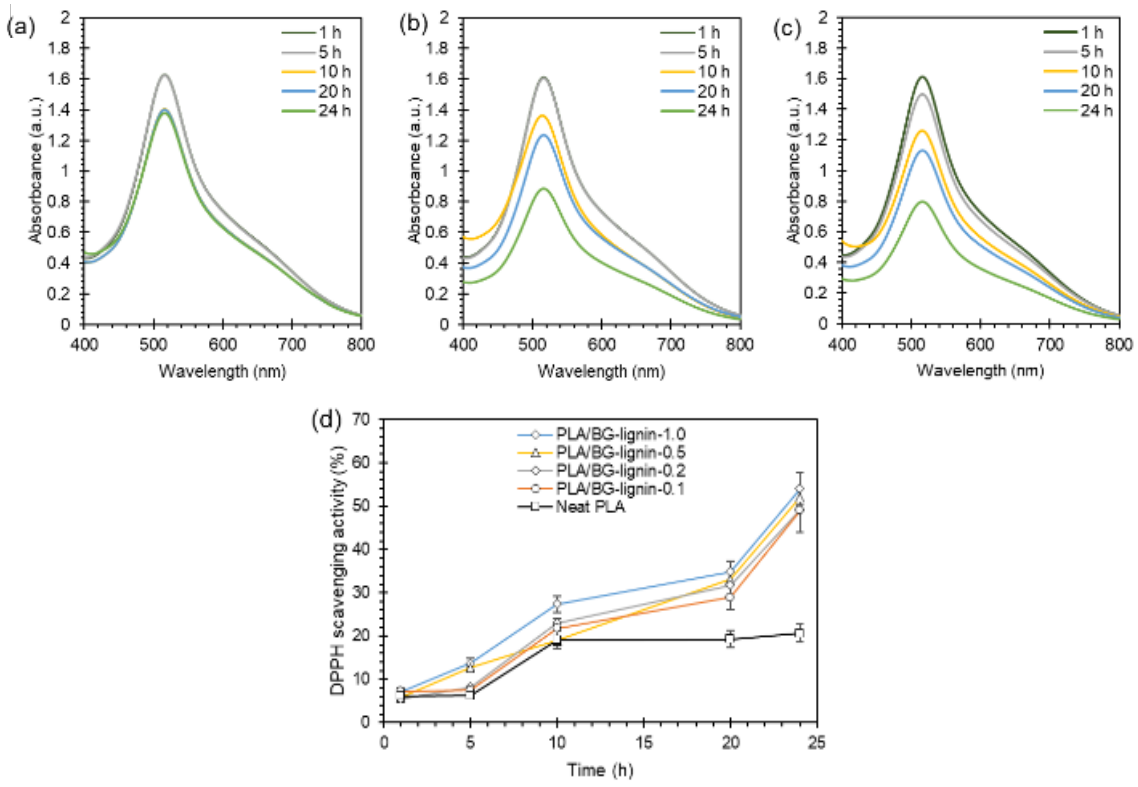

Figure 7. Absorption of the DPPH band at 517 nm of (a) neat PLA film, (b) PLA composite film at 0.1 wt% BG-lignin, (c) PLA composite film at 1.0 wt% BG-lignin, and (d) Free radical (DPPH) scavenging activity of neat PLA and BG-lignin/PLA composite films at different incubation periods.

Table 3. Overall migration values of neat PLA and its composite films containing BG-lignin.

Sample	Overall migration [mg·kg^{-1}]				
	Simulant A (Ethanol 10% (v/v))	**Simulant B (Acetic acid 3% (w/v))**	**Simulant C (Ethanol 20% (v/v))**	**Simulant D1 (Ethanol 50% (v/v))**	**Simulant D2 (n-heptane)**
Neat PLA	4.4 ± 3.1	7.4 ± 4.2	6.3 ± 1.0	5.6 ± 1.6	5.3 ± 2.2
PLA/BG-lignin_0.1	7.8 ± 8.3	-	-	7.3 ± 0.8	-
PLA/BG-lignin_0.2	11.2 ± 9.8	-	-	13.5 ± 1.6	-
PLA/BG-lignin_0.5	19.7 ± 26.2	-	-	10.1 ± 1.6	-
PLA/BG-lignin_1.0	43.5 ± 24.1	13.5 ± 1.54	4.9 ± 2.6	13.5 ± 1.6	11.2 ± 0.8

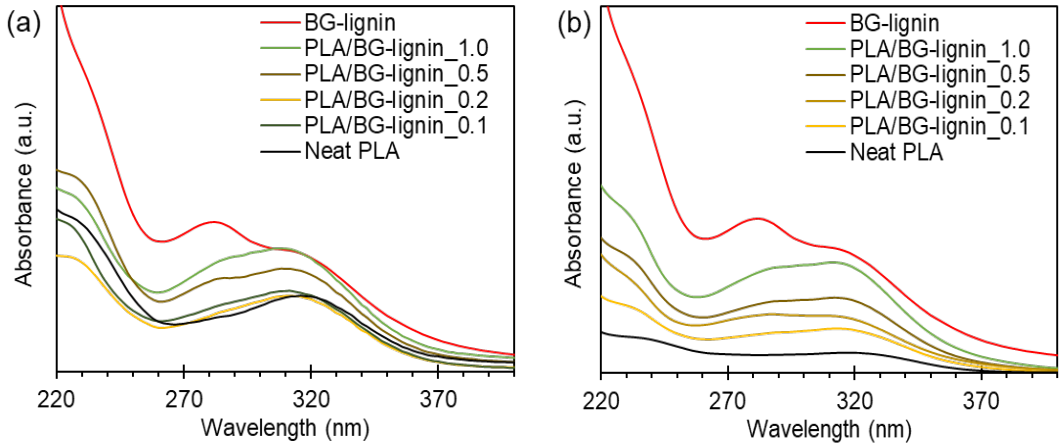

Figure 8. UV spectra of food simulant after 10 days of incubation: (a) food simulant A (Ethanol 10% (v/v)), and (b) simulant D1 (Ethanol 50% (v/v)).

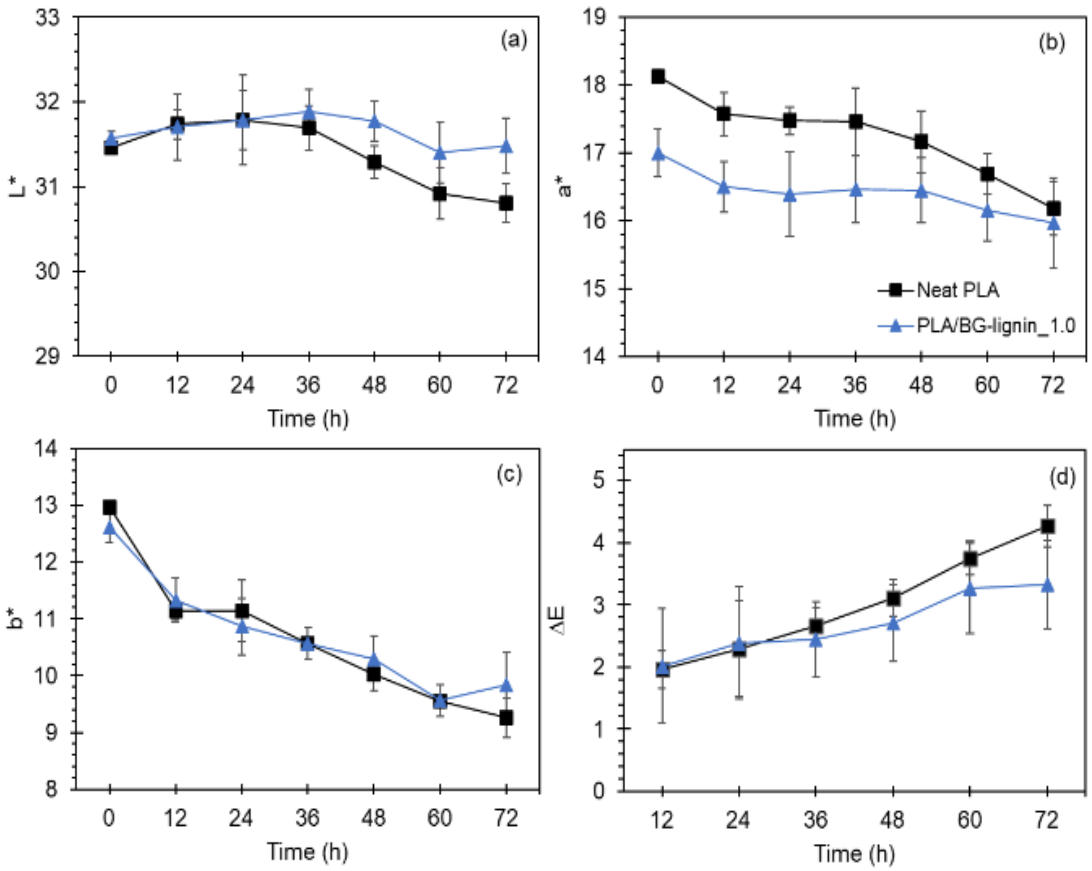

Figure 9. Color coordinates of ketchup contained in neat PLA and PLA/BG-lignin films, collected over a 72 h UV-irradiation period: (a) L*, (b) a*, (c) b* and (d) ΔE.

The in vitro cell cytotoxicity study was conducted on mouse fibroblast cells. Neat PLA and PLA/BG-lignin_1.0 films exhibited % viability at 94% and 96%, respectively. These values were larger the rejection criteria (70%), indicating both neat PLA and PLA containing BG-lignin at 1.0 wt% are non-cytotoxicity. Regarding the active properties of PLA film containing BG-lignin, which include UV-blocking and free radical scavenging capabilities, along with acceptable migration values and non-cytotoxicity, it becomes advantageous for applications in preventing photooxidation in food packaging. Tomato ketchup, a widely popular product, is susceptible to degradation due to exposure to ultraviolet (UV) light and temperature fluctuations [62,63]. Tomato ketchup was contained in different sachets made from neat PLA and PLA/BG-lignin_1.0, following a 72 h UV exposure. The effects of photooxidation on lycopene content enriched in tomato were assessed through color measurement.

Figure 9 illustrates the color data of tomato ketchup for 72 h exposed to UV irradiation. Ketchup contained in the neat PLA package exhibited a lower L* value and higher a* value compared to that contained in PLA/BG-lignin, as shown in Figure 9(a-b), indicating that the PLA/BG-lignin film can prevent changes in the lightness and red color of ketchup. Figure 9(c) shows the change in b* values for both types of packaging, which decreased similarly. Figure 9(d) illustrates a plot of ΔE values with UV exposure time. The ΔE values of ketchup stored in both neat PLA and PLA/BG-lignin exhibited comparable values of 2.0 after 12 h UV irradiation, signifying detectable color variation when the ΔE reaches this threshold. Subsequent to 72 h UV exposure, the ΔE value of ketchup stored in neat PLA surpassed 4.0, indicating a conspicuous color alteration that is easily observable. Conversely, the ΔE value of ketchup stored in PLA/BG-lignin remained below 3.0. A ΔE value above 3.0 generally indicates noticeable color change to the human eye. The ΔE values of ketchup stored in neat PLA exceeded this threshold after 72 h, while PLA/BG-lignin maintained ΔE below 3.0, indicating better visual stability [64]. UV light directly initiates the degradation of internal photosensitive components through photo-chemical reactions, prompting phenomena such as lipid oxidation, pigment deterioration, and the generation of off flavors [65]. This discrepancy is attributed to the incorporation of lignin in the packaging, which helps maintain the color of tomato ketchup or reduce color degradation after UV exposure, owing to its UV protection and anti-oxidation properties.

4. Conclusions

The utilization of organosolv BG-lignin extracted from Thai sugarcane bagasse as multifunctional bio-additives in PLA flexible films represents a promising avenue for enhancing the properties of packaging materials. Physicochemical attributes of BG-lignin, such as molecular weight, functional groups, and phenolic compounds, significantly contribute to UV-shielding and antioxidant activities, while its thermal properties facilitate melt extrusion processing. The addition of BG-lignin results in brownish PLA composite films with optical, thermal, and mechanical properties comparable to neat PLA film, demonstrating promising UV absorption and free radical scavenging capabilities. Furthermore, PLA/BG-lignin composite films comply with European migration legislative limits for food packaging materials and exhibit non-cytotoxicity. However, excessive loading content negatively affects film color. PLA film containing BG-lignin at 1.0 wt% effectively retards the photooxidation reaction causing color change in tomato ketchup. Overall, BG-lignin emerges as a versatile bio-additive for the development of practical and economically effective active packaging solutions. It is imperative to customize its loading content and UV-barrier qualities to suit individual application requirements.

Acknowledgements

The authors acknowledge resources and support by the National Science, Research and Innovation Fund (NSRF) - Fundamental Fund FY2025 via Thailand Science Research and Innovation (TSRI) and National Science and Technology Development Agency (NSTDA), Thailand (P2451214).

References

[1] Coversio Market and strategy, “Plastic flow 2018.” [Online]. Available: https://www.bkv-gmbh.de/files/bkv-neu/studien/Global_Plastics_Flow_Feb10_2020.pdf

[2] Plastic europe, “Plastics – the Facts 2020.”

[3] Bioplastics European, “Bioplastics facts and figures.” [Online]. Available:https://docs.european-bioplastics.org/publications/EUBP_Facts_and_figures.pdf

[4] Y. Kim, J. H. Seo, H. Seo, S. Kim, Y. Lee, K. Kim, and J. Lee, “All biomass and UV protective composite composed of compatibilized lignin and poly (lactic-acid),” *Scientific Reports*, vol. 7, pp. 6371-6381, 2017.

[5] J. Shojaeiarani, D. S. Bajwa, C. Ryan, and S. Kane, “Enhancing UV-shielding and mechanical properties of polylactic acid nanocomposites by adding lignin coated cellulose nanocrystals,” *Industrial Crops and Products*, vol. 183, p. 114904, 2022.

[6] K. Chi, and J. M. Catchmark, “Enhanced dispersion and interface compatibilization of crystalline nanocellulose in polylactide by surfactant adsorption,” *Cellulose*, vol. 24, pp. 4845-4860, 2017.

[7] P. Müller, J. Bere, E. Fekete, J. Móczó, B. Nagy, M. Kállay, B. Kállay, and B. Kállay, “Interactions, structure and properties in PLA/plasticized starch blends,” *Polymer*, vol. 103, pp. 9-18, 2016.

[8] W. Yang, Y. Weng, D. Puglia, G. Qi, W. Dong, J. Kenny, and P. Ma, “Poly(lactic acid)/lignin films with enhanced toughness and anti-oxidation performance for active food packaging,” *International Journal of Biological Macromolecules*, vol. 144, pp. 102-110, 2020.

[9] W. Yang, F. Dominici, E. Fortunati, J. M. Kenny, and D. Puglia, “Effect of lignin nanoparticles and masterbatch procedures on the final properties of glycidyl methacrylate-g-poly (lactic acid) films before and after accelerated UV weathering,” *Industrial Crops and Products*, vol. 77, pp. 833-844, 2015.

[10] J. Tian, Y. Kong, S. Qian, Z. Zhang, Y. Xia, and Z. Li, “Mechanically robust multifunctional starch films reinforced by surface-tailored nanofibrillated cellulose,” *Composites Part B: Engineering*, vol. 275, p. 111339, 2024.

[11] H. Sadeghifar, and A. Ragauskas, “Lignin as a UV Light blocker-a review,” *Polymers,* vol 15, p. 1134, 2020.

[12] A. J. Basbasan, B. Hararak, C. Winotapun, W. Wanmolee, P. Leelaphiwat, K. Boonruang, and W. Chinsirikul, "Emerging challenges on viability and commercialization of lignin in biobased polymers for food packaging: A review," *Food Packaging and Shelf Life*, vol. 34, p. 100969, 2022.

[13] M. Paulsson, and J. Parkås, "Review: Light-induced yellowing of lignocellulosic pulps – Mechanisms and preventive methods," *Bioresources*, vol. 7, p. 5995, 2012.

[14] J. Acosta, E. Figueroa-Espinoza, M. Los, and M. D. L. Á. la Rosa-Alcaraz, "Recent Progress in the Production of Lignin-based Sunscreens: A Review," *Bioresources*, vol. 17, pp. 3674-3701, 2022.

[15] P. Posoknistakul, C. Tangkrakul, P. Chaosuanphae, S. Deepentham, W. Techasawong, N. Phonphirunrot, S. Bairak, C. Sakdaronnarong, and N. Sakdaronnarong, "Fabrication and characterization of lignin particles and their ultraviolet protection ability in PVA composite film," *ACS Omega*, vol. 5, pp. 20976-20982, 2020.

[16] H. Faustino, N. Gil, C. Baptista, and A. P. Duarte, "Antioxidant Activity of Lignin Phenolic Compounds Extracted from Kraft and Sulphite Black Liquors," *Molecules*, vol. 15, pp. 9308-9322, 2010.

[17] B. Jiang, Y. Zhang, L. Gu, W. Wu, H. Zhao, and Y. Jin, "Structural elucidation and antioxidant activity of lignin isolated from rice straw and alkali oxygen black liquor," International *Journal of Biological Macromolecules*, vol. 116, pp. 513-519, 2018.

[18] X. Pan, J. F. Kadla, K. Ehara, N. Gilkes, and J. N. Saddler, "Organosolv ethanol lignin from hybrid poplar as a radical scavenger: Relationship between lignin structure, extraction conditions, and antioxidant activity," *Journal of Agricultural and Food Chemistry*, vol. 54, pp. 5806-5813, 2006.

[19] F. G. Calvo-Flores, J. A. Dobado, J. Isac-García, and F. J. Martín-Martínez, "Lignin and lignans as renewable raw materials: chemistry, technology and applications," John Wiley & Sons Ltd, 2015.

[20] J. F. Leal Silva, P. Y. S. Nakasu, A. C. da Costa, R. Maciel Filho, and S. C. Rabelo, "Techno-economic analysis of the production of 2G ethanol and technical lignin via a protic ionic liquid pretreatment of sugarcane bagasse," *Industrial Crops and Products*, vol. 189, p. 115788, 2022.

[21] T. L. Bezerra, and A. J. Ragauskas, "A review of sugarcane bagasse for second-generation bioethanol and biopower production," *Biofuels, Bioproducts and Biorefining*, vol. 10, pp. 634-647, 2016.

[22] S. Pongchaiphol, N. Suriyachai, B. Hararak, M. Raita, N. Laosiripojana, and V. Champreda, "Physicochemical characteristics of organosolv lignins from different lignocellulosic agricultural wastes," *International Journal of Biological Macromolecules*, vol. 216, pp. 710-727, 2022.

[23] S. Y. Park, J.-Y. Kim, H. J. Youn, and J. W. Choi, "Utilization of lignin fractions in UV resistant lignin-PLA biocomposites via lignin-lactide grafting," *International Journal of Biological Macromolecules*, vol. 138, pp. 1029-1034, 2019.

[24] C. Ma, T.-H. Kim, K. Liu, M.-G. Ma, S.-E. Choi, and C. Si, "multifunctional lignin-based composite materials for emerging applications," *Frontiers in Bioengineering and Biotechnology*, vol. 9, 2021.

[25] Y. Kim, J. Suhr, H-W. Seo, H. Sun, S. Kim, I-K. Park, S-H. Kim, Y. Lee, K-J. Kim, and J-D. Nam, "All biomass and UV protective composite composed of compatibilized lignin and poly (lactic-acid)," *Scientific Reports,* vol. 7, p. 43596, 2017.

[26] S. R. Yearla, and K. Padmasree, "Preparation and characterisation of lignin nanoparticles: evaluation of their potential as antioxidants and UV protectants," *Journal of Experimental Nanoscience*, vol. 11, pp. 289-302, 2016.

[27] X. Meng, C. Crestini, H. Ben, N. Hao, Y. Pu, A. Ragauskas, and D. Argyropoulos "Determination of hydroxyl groups in biorefinery resources via quantitative 31P NMR spectroscopy," *Nature Protocols*, vol. 14, pp. 2627-2647, 2019.

[28] D. Araújo, I. da Cruz Filho, T. Santos, D. Pereira, D. Marques, A. da Conceição Alves de Lima, T. de Aquino, G. de Moraes Rocha, M. do Carmo Alves de Lima, and F. Nogueira, "Biological activities and physicochemical characterization of alkaline lignins obtained from branches and leaves of Buchenavia viridiflora with potential pharmaceutical and biomedical applications," *International Journal of Biological Macromolecules,* vol. 219, pp. 224-245, 2022.

[29] X. Zhou, X. Liu, Q. Wang, G. Lin, H. Yang, D. Yu, S. Cui, and W. Xia, "Antimicrobial and antioxidant films formed by bacterial cellulose, chitosan and tea polyphenol – Shelf life extension of grass carp," *Food Packaging and Shelf Life*, vol. 33, p. 100866, 2022.

[30] P. Terzioğlu, F. Güney, F. N. Parın, İ. Şen, and S. Tuna, "Biowaste orange peel incorporated chitosan/polyvinyl alcohol composite films for food packaging applications," *Food Packaging and Shelf Life*, vol. 30, p. 100742, 2021.

[31] G. Cazacu, R. Darie-Nita, O. Chirila, M. Totolin, M. Asandulesa, D. Ciolacu, J. Ludwiczak, and C. Vasile, "Environmentally friendly polylactic acid/modified lignosulfonate biocomposites," *Journal of Polymers and the Environment*, vol. 25, no. 3, pp. 884-902, 2017.

[32] K. Crouvisier-Urion, P. Bodart, P. Winckler, J. Raya, R. Gougeon, P. Cayot, S. Domenek, F. Debeaufort, and T. Karbowiak, "Biobased composite films from chitosan and lignin: antioxidant activity related to structure and moisture," *ACS Sustainable Chemistry & Engineering*, vol. 4, pp. 6371-6381, 2016.

[33] L. Valencia, E. M. Nomena, A. P. Mathew, and K. P. Velikov, "Biobased cellulose nanofibril–oil composite films for active edible barriers," *ACS Applied Materials & Interfaces*, vol. 11, pp. 16040-16047, 2019.

[34] E. S. Esakkimuthu, D. DeVallance, I. Pylypchuk, A. Moreno, and M. H. Sipponen, "Multifunctional lignin-poly (lactic acid) biocomposites for packaging applications," *Frontiers in Bioengineering and Biotechnology*, vol. 10, 2022.

[35] H. Sun, G. Wang, J. Ge, N. Wei, W. Sui, Z. Chen, H. Jia, A. M. Parvez, and C. Si, "Reduction of lignin heterogeneity for improved catalytic performance of lignin nanosphere supported Pd nanoparticles," *Industrial Crops and Products*, vol. 180, p. 114685, 2022.

[36] M. R. V. Bertolo, L. B. Brenelli de Paiva, V. M. Nascimento,

C. A. Gandin, M. O. Neto, C. E. Driemeier, and S. C. Rabelo, "Lignins from sugarcane bagasse: Renewable source of nanoparticles as Pickering emulsions stabilizers for bioactive compounds encapsulation," *Industrial Crops and Products*, vol. 140, p. 111591, 2019.

[37] J. H. Choi, S.-M. Cho, J.-C. Kim, S. W. Park, Y.-M. Cho, B. Koo, H. W. Kwak, and I.-G. Choi, "Thermal properties of ethanol organosolv lignin depending on its structure," *ACS Omega*, vol. 6, pp. 1534-1546, 2021.

[38] P. Wannid, B. Hararak, S. Padee, W. Klinsukhon, N. Suwannamek, M. Raita, K. Khao-on, and C. Prahsarn, "Structural and thermal characteristics of novel organosolv lignins extracted from thai biomass residues: A guide for processing," *Journal of Polymers and the Environment*, vol. 8, p. 860, 2022.

[39] F. Monteil-Rivera, M. Phuong, M. Ye, A. Halasz, and J. Hawari, "Isolation and characterization of herbaceous lignins for applications in biomaterials," *Industrial Crops and Products*, vol. 41, pp. 356-364, 2013.

[40] F. Gomes, R. de Souza, E. Brito, and R. Lelis, "A review on lignin sources and uses," *Journal of Applied Biotechnology & Bioengineering*, pp. 100-105, 2020.

[41] Y. Zhang and M. Naebe, "Lignin: A review on structure, properties, and applications as a light-colored UV absorber," *ACS Sustainable Chemistry & Engineering*, vol. 9, pp. 1427-1442, 2021.

[42] Y. Guo, D. Tian, F. Shen, G. Yang, L. Long, J. He, C. Song, J. Zhang, Y. Zhu, C. Huang, and S. Deng, "Transparent cellulose/technical lignin composite films for advanced packaging," *Polymers*, vol. 11, p. 1455, 2019.

[43] I. Brodin, M. Ernstsson, G. Gellerstedt, and E. Sjöholm, "Oxidative stabilisation of kraft lignin for carbon fibre production," *Holzforschung*, vol. 66, pp. 141-147, 2012.

[44] I. Norberg, Y. Nordström, R. Drougge, G. Gellerstedt, and E. Sjöholm, "A new method for stabilizing softwood kraft lignin fibers for carbon fiber production," *Journal of Applied Polymer Science*, vol. 128, pp. 3824-3830, 2013.

[45] Y. Nordström, I. Norberg, E. Sjöholm, and R. Drougge, "A new softening agent for melt spinning of softwood kraft lignin," *Journal of Applied Polymer Science*, vol. 129, pp. 1274-1279, 2013.

[46] J. L. Braun, K. M. Holtman, and J. F. Kadla, "Lignin-based carbon fibers: Oxidative thermostabilization of kraft lignin," *Carbon*, vol. 43, pp. 385-394, 2005.

[47] H. Mainka, L. Hilfert, S. Busse, F. Edelmann, E. Haak, and A. S. Herrmann, "Characterization of the major reactions during conversion of lignin to carbon fiber," *Journal of Materials Research and Technology*, vol. 4, pp. 377-391, 2015.

[48] F. Antunes, I. F. Mota, J. da Silva Burgal, M. Pintado, and P. S. Costa, "A review on the valorization of lignin from sugarcane by-products: From extraction to application," *Biomass Bioenergy*, vol. 166, p. 106603, 2022.

[49] B. Jiang, Y. Zhang, H. Zhao, T. Guo, W. Wu, and Y. Jin, "Structure-antioxidant activity relationship of active oxygen catalytic lignin and lignin-carbohydrate complex," *International Journal of Biological Macromolecules*, vol. 139, pp. 21-29, 2019.

[50] S. H. Fasihnia, S. H. Peighambardoust, S. J. Peighambardoust, A. Oromiehie, M. Soltanzadeh, and D. Peressini, "Migration analysis, antioxidant, and mechanical characterization of polypropylene-based active food packaging films loaded with BHA, BHT, and TBHQ.," *Journal of Food Science*, vol. 85, pp. 2317-2328, 2020.

[51] H. Ortiz-Vazquez, J. Shin, H. Soto-Valdez, and R. Auras, "Release of butylated hydroxytoluene (BHT) from Poly(lactic acid) films," *Polymer Testing*, vol. 30, pp. 463-471, 2011.

[52] R. Kaur, and S. K. Uppal, "Structural characterization and antioxidant activity of lignin from sugarcane bagasse," *Colloid and Polymer Science*, vol. 293, pp. 2585-2592, 2015.

[53] R. Kaur, S. K. Uppal, and P. Sharma, "Antioxidant and antibacterial activities of sugarcane bagasse lignin and chemically modified lignins," *Sugar Tech*, vol. 19, pp. 675-680, 2017.

[54] H. Kargarzadeh, A. Galeski, and A. Pawlak, "PBAT green composites: Effects of kraft lignin particles on the morphological, thermal, crystalline, macro and micromechanical properties," *Polymer*, vol. 203, p. 122748, 2020.

[55] E. M. Zadeh, S. F. O'Keefe, and Y. T. Kim, "Utilization of lignin in biopolymeric packaging films," *ACS Omega*, vol. 3, pp. 7388-7398, 2018.

[56] F. Xiong, Y. Wu, G. Li, Y. Han, and F. Chu, "Transparent nanocomposite films of lignin nanospheres and poly(vinyl alcohol) for UV-absorbing," *Industrial & Engineering Chemistry Research*, vol. 57, pp. 1207-1212, 2018.

[57] X. Zhang, W. Liu, W. Liu, and X. Qiu, "High performance PVA/lignin nanocomposite films with excellent water vapor barrier and UV-shielding properties," *International Journal of Biological Macromolecules*, vol. 142, pp. 551-558, 2020.

[58] J. Gómez-Estaca, C. López-de-Dicastillo, P. Hernández-Muñoz, R. Catalá, and R. Gavara, "Advances in antioxidant active food packaging," *Trends in Food Science & Technology*, vol. 35, pp. 42-51, 2014.

[59] A. J. Basbasan, B. Hararak, C. Winotapun, W. Wanmolee, P. Leelaphiwat, K. Boonruang, W. Chinsirikul, and V. Chonhenchob, "Emerging challenges on viability and commercialization of lignin in biobased polymers for food packaging: A review," *Food Packaging and Shelf Life*, vol. 34, p. 100969, 2022.

[60] M. Hosseini, L. Moghaddam, L. Barner, S. Cometta, D. W. Hutmacher, and F. Medeiros Savi, "The multifaceted role of tannic acid: From its extraction and structure to antibacterial properties and applications," *Progress in polymer science*, vol. 160, p. 101908, 2025.

[61] R. A. Lee, C. Bédard, V. Berberi, R. Beauchet, and J.-M. Lavoie, "UV–Vis as quantification tool for solubilized lignin following a single-shot steam process," *Bioresource Technology*, vol. 144, pp. 658-663, 2013.

[62] N. Kohan-Nia, R. Mahmoudi, and B. Pakbin, "Effect of packaging material on color properties of catsup tomato sauce." *Journal of Applied Packaging Research*, vol 8, pp. 10-16, 2016.

[63] A. Rajchl, M. Voldřich, H. Čížková, M. Hronová, R. Ševčík, J. Dobiáš, and J. Pivoňka, "Stability of nutritionally important compounds and shelf life prediction of tomato ketchup," *Journal of Food Engineering*, vol. 99, pp. 465-470, 2010.

[64] G. Sharma, W. Wu, and E. N. Dalal, "The CIEDE2000 color-difference formula: Implementation notes, supplementary test data, and mathematical observations," *Color Research an Application*, vol. 30, pp. 21-30, 2005.

[65] Y. Zhang, and W. Jiang, "Effective strategies to enhance ultraviolet barrier ability in biodegradable polymer-based films/coatings for fruit and vegetable packaging," *Trends in Food Science & Technology*, vol 139, p. 104139, 2023.